

Published in final edited form as:

*Biomaterials*. 2007 October ; 28(28): 4132–4142. doi:10.1016/j.biomaterials.2007.05.035.

## Self-assembled polyethylenimine-graft-poly( $\epsilon$ -caprolactone) micelles as potential dual carriers of genes and anticancer drugs

Li Yan Qiu<sup>a,b</sup> and You Han Bae<sup>a,\*</sup>

<sup>a</sup> Department of Pharmaceutics and Pharmaceutical Chemistry, University of Utah, 421 Wakara Way, Suite 315, Salt Lake City, UT 84108, USA

<sup>b</sup> College of Pharmaceutical Sciences, Zhejiang University, Hangzhou 310058, China

### Abstract

A series of amphiphilic cationic graft polymers (PEC) were synthesized by coupling poly( $\epsilon$ -caprolactone) of differing molecular weights (MW) to low MW branched polyethylenimine via an amide group. IR, <sup>1</sup>H-NMR and GPC were employed to characterize the graft copolymers. The self-assembly characteristics of these copolymers in an aqueous solution were studied by fluorescence techniques. The critical micelle concentration (CMC) varied from 0.044 to 0.032 g/L when the MW of poly( $\epsilon$ -caprolactone) increased from 1800 to 5500. The micelles formed electrostatic complexes with a reporter gene (pCMV-Luc) after an anticancer drug, Doxorubicin (DOX), was loaded by dialysis method. Gel retardation studies proved that micelles with or without Dox were able to complex with DNA completely at an equivalent N/P ratio of around 2.0, indicating that drug loading did not interfere in the interaction between the PEI shell and DNA. Particle size slightly decreased at higher N/P ratios of polyplexes, but increased with drug encapsulation. It was also noted that DNA/micelle complexes were significantly less toxic to HepG2 cells than blank PEC micelles, and improved gene transfection efficiency (about 3 orders of magnitude greater than PEI 25K alone at most) whether DOX was present in the system or not. These results suggest that this group of cationic graft polymers may be a potential candidate for the development of a drug delivery system that can examine the synergistic effects of combined drug and gene therapy.

### Keywords

Gene therapy; Doxorubicin; Polyethylenimine; Poly( $\epsilon$ -caprolactone); Graft copolymer

## 1. Introduction

Chemotherapy is presently employed as one of the frontline approaches along with surgery and radiation therapy to treat cancers in the clinic. However, its application is always accompanied by inevitable side effects including suppression of bone marrow and other fast dividing tissues and induction of secondary cancer occurrences. More seriously, long-term chemotherapy causes the development of resistant cell phenotypes, resulting in the loss of sensitivity of cancer cells to anticancer agents. To date, targeting concepts have been well established based on the development of nanotechnology and physical feature of tumor tissue.

\*Corresponding author. E-mail address: E-mail: you.bae@utah.edu.

**Publisher's Disclaimer:** This is a PDF file of an unedited manuscript that has been accepted for publication. As a service to our customers we are providing this early version of the manuscript. The manuscript will undergo copyediting, typesetting, and review of the resulting proof before it is published in its final citable form. Please note that during the production process errors may be discovered which could affect the content, and all legal disclaimers that apply to the journal pertain.

Specific antibodies or ligands linkage and thermo- or pH-responsive modification on polymeric carriers have been explored to increase drug accumulation and release at tumor sites [1,2]. Comparatively, an advance in addressing the problem of multidrug resistance (MDR) is quite limited from the viewpoint of drug delivery system design. Polyisohexacyanoacrylate nanospheres [3–6], pluronic micelles [7–9] and liposomes [10–11] were mostly tried to reverse drug resistance probably by bypassing P-glycoprotein (P-gp) of which over-expression is associated with the development of MDR in cancer cells. On the other side, various attempts have been made to overcome MDR at a gene level. Kabayashi et al. developed anti-MDR1 hammerhead ribozymes driven by the  $\beta$ -actin promoter. Upon retroviral-mediated transfer of anti MDR1 ribozyme into human leukemia cell lines expressing MDR1, partial reversal of vincristine resistance as well as reduction of MDR1 mRNA and P-gp protein levels were found [12]. Similarly, Gao and colleagues constructed a retroviral vector containing anti-MDR1 ribozyme coupled to the carcinoembryonic-antigen (CEA) promoter and introduced the vector into resistant colon-cancer cells (SW1116R) that produce CEA. The expression of MDR1 mRNA and P-gp decreased significantly and drug resistance to DOX decreased 93 % [13]. Another alternative approach was to enhance their chemosensitivity by introducing wild-type *p53*, a tumor suppressor gene, into mutant *p53* cells since over-production of Pgp is often closely related to mutant *p53* [14]. Using this method, the 50 % inhibitory concentration (IC<sub>50</sub>) of DOX for the SKLMS-1 wt *p53* transfectants decreased 16-fold compared with SKLMS-1 parental cells expressing mutant *p53* [15]. Also Ulrike Stein et al. first linked cytokine gene transduction and MDR to increase the chemosensitivity of doxorubicin and vincristine in 1996 [16]. Hence, gene therapy displays the potential to treat MDR cancer cells effectively.

Herein a novel therapy strategy to circumvent MDR has been conceived on the basis of combining chemical and gene therapy together. When a chemical therapeutic is administered, certain genes can be delivered to cancer cells simultaneously with the aim to keep targeted cells sensitive to drug during the entire treatment period. A unique example of the co-delivery of paclitaxel and DNA or siRNA has recently been reported [17]. The synthetic polycations modified with cholesteryl groups that form self-assembled nanoparticles were used as the carrier. In our study, a series of amphiphilic poly( $\epsilon$ -caprolactone) (PCL) grafted branched polyethylenimine (PEI) were synthesized to form micellar carriers, where PEI would act as a complexing site with DNA through electrostatic interactions as well as the hydrophilic shell of the self-assembled micelles, while PCL constructed a hydrophobic core to encapsulate hydrophobic anticancer drugs. Branched PEI has been studied extensively as a non-viral gene carrier and become the standard of non-viral gene delivery because of its excellent transfection efficiency. Though it was reported linear PEI 22kDa displayed excellent transfection efficiency with a rather low toxicity [18], the protein expression capability of small linear PEI is evidently lower than that of small branched PEI [19]. In addition, as generally recognized, the toxicity of branched PEI decreases with the decrease of molecular weight [20]. Thus branched PEI with low molecular weight of 1.8k was chosen in this delivery system. Besides, the relationship among polymer structure, drug loading and gene transfection was discussed in detail. In order to demonstrate the proposed concept clearly, a model reporter gene, luciferase, was selected in this study with the emphasis on gene transfection in the early phase of incubation rather than DOX cytotoxicity.

## 2. Experimental Methods

### 2.1. Materials

Branched polyethylenimines (PEI) with MWs of 1800 (99 %) and 25,000 (PEI 25K) were purchased from Polysciences Inc. (Warrington, PA, USA).  $\epsilon$ -Caprolactone (CL), stannous (II) octoate (SnOct), succinic anhydride, dicyclohexyl carbodiimide (DCC), 4-(dimethyl amino) pyridine (DMAP), and triethylamine (TEA) were obtained from Aldrich and used as received.

Dioxane and dichloroform (Aldrich) were dried over  $\text{CaH}_2$ , and distilled before use. Dulbecco's phosphate buffered saline (DPBS), Dulbecco's modified Eagle's medium (DMEM), bovine serum albumin (BSA), 3-(4,5-dimethylthiazol-2-yl)-2,5-diphenyl tetrazolium bromide (MTT) were purchased from Sigma Chemicals Co. (St. Louis, Mo). 4-(2-Hydroxy-ethyl)-1-piper-azine ethanesulfonic acid (HEPES) and fetal bovine serum were supplied by GIBCO BRL (Grand Island, NY). Doxorubicin hydrochloride (DOX·HCl) was kindly provided by Boryung Pharm. Co. (Korea). BCA™ protein assay kits (Cat.#23225) and ethidium bromide (Rockford, IL) were purchased from Pierce Biotechnology. Agarose and Luciferase assay kits were obtained from Promega Co. (Madison, WI). Plasmid DNA containing the firefly luciferase reporter gene (pCMV-Luc) was purchased from Elim Biopharmaceuticals, Inc. (San Francisco, CA, USA).

## 2.2. Synthesis of polyethylenimine-graft-poly( $\epsilon$ -caprolactone) (PEC)

Monohydroxy-terminated PCL (PCL-OH) was first synthesized by ring-opening polymerization of CL using benzyl alcohol (BA) as an initiator and SnOct as a catalyst (0.1 % moles of CL monomer) according to the reference [21]. CL, SnOct and BA were weighed into a dry round-bottom flask. Under constant stirring, polymerization was carried out in dry nitrogen atmosphere at 115°C for 24 hr. The product was precipitated in cold methanol from dichloromethane and vacuum-dried. The polymerization degree was controlled by the feed ratio of BA to CL.

Monocarboxy-capped PCL (PCL-COOH) was prepared through hydroxyl esterification with succinic anhydride. In brief, PCL-OH (0.1mmol hydroxyl group), succinic anhydride (20 mg, 0.2 mmol), and 4-dimethyl amino pyridine (DMAP) (24.4 mg, 0.2 mmol) were dissolved in dry dioxane [22]. After 24 hr, the solution was filtered, condensed and precipitated in ether to obtain polymer powder. This crude product was re-dissolved in dichloroform and washed three times with aqueous hydrochloric acid (10 v/v%) and then three times with a saturated NaCl solution. The organic phase was separated, dried with magnesium sulfate over night and filtered. PCL-COOH was collected by precipitation into ether and vacuum-dried. The reaction yield was over 80 %.

PEI (0.72 g, 0.4 mmol), PCL-COOH (0.1 mmol carboxyl group), DMAP (48.8 mg, 0.4 mmol) and DCC (82.5 mg, 0.4 mmol) were dissolved in dry dichloromethane and reacted for three days under constant stirring. Methanol was added into the mixture until a clear solution was obtained. This solution was transferred into a dialysis tube (Spectrapore, MWCO 10,000) and immersed in 500ml dichloroform with mild shaking for two days. The mixture in the dialysis membrane was then vacuum-dried and re-dissolved in fresh methanol. The polymer was recovered by filtration and precipitation in ether, and further purified by re-dissolving in water and dialysis against water for two days to remove any unreacted PEI. After filtering through a 0.8- $\mu\text{m}$  microporous membrane, the dialysis solution was freeze-dried to obtain the resultant polymer. The reaction yield was about 75 %. The chemical structure of the resultant polymers was confirmed by  $^1\text{H}$  NMR spectroscopy (Varian Mercury 400) and IR. GPC was performed using a Waters 515 HPLC pump and a Waters 2410 refractive index detector. THF was used as the solvent with a flow rate of 1.5 mL/min at 40°C and narrow disperse polystyrenes served as calibration standards.

## 2.3. Determination of critical micelle concentration (CMC)

Sample solutions for fluorescence investigation were prepared as described previously [23]. Briefly, a known amount of pyrene in THF was added to each of a series of 10 ml vials and THF was evaporated. The final concentration of pyrene was  $6.0 \times 10^{-7}$  M. A total of 5 mL of various concentrations of aqueous polymer solutions were added to each vial and then heated

at 45°C for 3 hr to equilibrate pyrene with the micelles, and left to cool for 3 hr at room temperature.

Steady-state fluorescent spectra were measured using an F-4500 fluorescence spectrophotometer (Hitachi High-Technologies Co., Tokyo, Japan) with a slit width of 2.5 nm for emission. For fluorescence emission spectra, excitation wavelength was set at 339 nm, and for excitation spectra, the emission wavelength was 390 nm. Spectra were acquired with a scan speed of 240 nm min<sup>-1</sup>. All experiments were carried out at room temperature.

#### 2.4. Preparation of drug-loaded micelles

DOX·HCl (20 mg) was dissolved in 3 mL methanol/water (2:1) in the presence of TEA (1.5 times molar quantity of DOX) to form a free DOX-containing solution, which was then mixed with 1 mL of methanol solution with various polymer concentrations. This solution was transferred into a dialysis tube (Spectrapore, MWCO 10,000) to dialyze against distilled water for 48 hr. The outer solution was exchanged at appropriate time intervals. After filtration through a 0.8- $\mu$ m microporous membrane, the dialysis solution was freeze-dried to obtain the resultant drug-loaded micelles. Drug loading content was determined spectrophotometrically by measuring the absorption of the lyophilized sample dissolved in DMSO at a wavelength of 481 nm.

#### 2.5. Preparation of polyplexes

The preparation of DNA/micelle or drug-loaded DNA/micelle complexes was required before performing gel retardation studies, particle size and zeta potential measurements, gene transfection and cell viability tests. Generally, a series of PEC micelle or drug-loaded PEC micelle solutions with varying micelle concentration were prepared by dissolving micelles in deionized water first. After adding a calculated amount of DNA to each vial, the mixture was vortexed for 15 seconds and kept still at room temperature for 30 min. As a result, a series of polyplexes were formed with different N/P ratios.

#### 2.6. Gel retardation study

The formed polyplex solution (15  $\mu$ L) was mixed with 3  $\mu$ L loading dye (Nalgene 2100), and loaded into a 1% agarose gel containing ethidium bromide (500 ng/mL). Electrophoresis was set up in TAE buffer at 100 mV and kept for 60 min. The gel was viewed using a UV transilluminator.

#### 2.7. Particle size and zeta potential measurements

Polyplex solutions (2 mL) were prepared as described above and the concentration of micelles was fixed at 0.05 mg/mL in deionized water. Zeta potential and particle size were measured using a Zetasizer 3000HS (Malvern Instrument, Inc., Worcestershire, UK) at a wavelength of 677 nm with a constant angle of 90°C at room temperature.

#### 2.8. Cell viability

The cell cytotoxicity of PEC micelles, drug-loaded PEC micelles and DNA/PEC micelle complexes with or without drug was examined by MTT assay according to standard protocols. HepG2 cells (hepatoma cells) were seeded in a 96-well plate at a density of  $1 \times 10^5$  cells/well in 0.1 mL DMEM media supplemented with 10% FBS and incubated for 24 hr at 37°C in 5% CO<sub>2</sub>. Six unseeded wells were set as a control group. Then 25  $\mu$ L of sample solution at different concentrations was added to each well and incubated for 4 hr. 31.3  $\mu$ L of MTT stock solution (5 mg/mL in PBS) was added into each well for a final concentration of 1 mg/mL MTT and incubated for 3 hr. The media was completely removed, 200  $\mu$ L of DMSO was added to dissolve the formazan crystals formed by viable cells, and the system was incubated at 37°C for 10 min.

Percentage of cell viability was calculated from the absorbance at 570 nm using a microplate reader (SpectraMax ® M2; Molecular Device).

## 2.9. In vitro transfection study

HepG2 cells were seeded at a density of  $5 \times 10^5$  cells/well in DMEM media supplemented with 10 % FBS in 24-well plates and cultured for 24 hr. Before adding various complex samples, the serum-containing culture medium was replaced with 1 mL of serum-free medium. Various complexes at different N/P ratios were added (100  $\mu$ L in water, containing 1  $\mu$ g DNA/well), and incubated with the cells for 4 hr at 37 °C. The medium was then replaced with 1 mL of fresh complete medium and the cells were incubated for an additional 44 hr. Transfection tests were performed in triplicate. After incubation, the medium was removed and the cells were rinsed once with DPBS. The cells in each well were treated with 200  $\mu$ L of 1X cell lysis buffer (Promega Co., Madison, WI) followed by freeze-thaw cycles three times to ensure complete lysis. The cell lysate was transferred into a 1 mL centrifuge vial and centrifuged for 5 min at 12,000 rpm and the supernatant was collected for luminescence measurements. Following the manufacturer's protocol for luciferase assay (Promega, Msdison, WI, Technical Bylletin), relative luminescent units (RLU) were evaluated by Plate Lumino Luminescence Analyzer (Strattec biomedical systems). Protein content in the cells was determined using BCA protein assay kit (Pierce, USA). Gene transfection efficiency is presented as RLU/mg protein.

## 3. Results and discussion

### 3.1. Polymer synthesis and characterization

Branched PEI grafted with PCL were synthesized by coupling carboxyl-terminated PCL of three different MWs to the amino groups of PEI in the presence of DMAP and DCC. The synthesis route is shown in Scheme 1. The MW of the PCL block in the copolymers was controlled by the molar feed ratio of the monomer CL to the initiator BA as shown in Table 1. The polymerization degree and MW of the corresponding PCL were calculated via the integration ratio of peaks at 1.31–1.37 ( $-\text{CH}_2-$ ) with those at 5.0 ( $-\text{CH}_2-\text{C}_6\text{H}_5$ ). Since branched PEI bears a number of primary and secondary amino groups, the conjugation of PEI with PCL was quite heterogeneous. After the reaction was completed, the resultant mixture was separated into two fractions by extraction with methanol. It was found that the compound dissolved in methanol was water-soluble while the other part was water-insoluble, which probably resulted from the different content of PCL in the copolymers. IR results support this theory. As shown in Fig. 1(a), the strong peak at  $1726 \text{ cm}^{-1}$  was assigned to the ester groups of PCL-OH. PEI was characterized by the broad band of primary, secondary, and tertiary amine groups at around  $3200\text{--}3500 \text{ cm}^{-1}$ , and absorption at  $1582 \text{ cm}^{-1}$  and  $1472 \text{ cm}^{-1}$  was assigned to the amine end groups ( $\nu_{\text{C-N}}$  and  $\nu_{\text{N-H}}$ ) (Fig. 1(b)). Compared to Figure 1(d), the spectrum in Figure 1(c) exhibited much stronger absorption at  $\sim 1726 \text{ cm}^{-1}$ , but much weaker absorption at around  $3200\text{--}3500 \text{ cm}^{-1}$ ,  $1582 \text{ cm}^{-1}$  and  $1472 \text{ cm}^{-1}$ . These differences suggest that more PCL blocks exist in the methanol-insoluble fraction while the methanol-soluble copolymer bears more available amine groups. Considering the aim to construct DNA-complexing vectors, the water-soluble PEC fractions were used for further studies. The chemical structure of PEC was further confirmed by  $^1\text{H-NMR}$  in  $d_6\text{-DMSO}$ . Fig. 2 presents the detailed assignments of  $^1\text{H-NMR}$  spectrum of PEC18. The  $^1\text{H-NMR}$  spectra of the other PECs had similar characteristics. The graft ratio, defined as the number of PCL chains per PEI molecule, could be determined from the ratio of the peak area corresponding to the methyl group in the PCL block to that of the methyl group in the PEI. The graft ratios of PEC were close to 1.0, suggesting almost one PCL with different MW was grafted onto one PEI molecule. Based on the graft ratio, the MW of PEC was obtained. These graft ratios were also supported by the fact that the MW of PEC measured by GPC was close to these values (Table 1).



### 3.2. Micellization behaviors and drug encapsulation

The self-association behavior of PEC was tested by a steady-state fluorescent probe study. Pyrene was chosen as the fluorescent probe because pyrene preferentially partitions into hydrophobic microdomains with a concurrent change in the molecule's photophysical properties. In the excitation spectra of pyrene in the presence of PEC18, fluorescent intensity was enhanced as PEC concentration increased. In addition, a red shift of excitation peaks was observed. All polymers exhibited similar characteristics in the excitation spectra. The plots of the intensity ratio  $I_{338}/I_{333}$  from excitation spectra are shown in Fig. 3 as a function of the PEC concentration. As reported by Wilhelm et al., the concentration dependence of the  $I_{338}/I_{333}$  ratios of pyrene is sensitive to a true onset of aggregation [24]. The value of  $I_{338}/I_{333}$  ratio increased significantly with the transfer of pyrene molecules from a polar to a more hydrophobic microdomain. As one can see, the plot of  $I_{338}/I_{333}$  vs.  $\log C$  is flat at low copolymer concentrations and sigmoidal in the crossover region. The critical micelle concentration (CMC) was determined from the intersection point of two straight lines: one line drawn through the points at the lowest polymer concentrations and another line through the points along the rapidly rising part of the plot. CMC thus obtained was about 0.044 mg/mL for PEC18 (Fig.3 (a)). Similarly, CMCs were 0.039 and 0.032 mg/mL for PEC 40 and PEC55, respectively. Thus increasing the hydrophobic segments to a certain degree would facilitate micellization of amphiphilic polymers [25].

Drug encapsulation was accompanied by micelle formation using a dialysis method. TEA was added to the DMSO before the drug solution was mixed with the PEC solution to remove hydrochloride in the drug [26]. In order to achieve high incorporation of DOX, TEA with 1.5 times equivalent to DOX·HCl was used. The relationship between the feed ratio of drug to PEC and drug loading was investigated. As shown in Table 2, the drug loading content increased as the drug feed increased for PEC18. The same effect was observed for PEC40 and PEC55. This result indicates that the DOX located in the micelle core helps further incorporation of DOX in the micelle [27]. However, there is no obvious difference among various PECs at the same drug/PEC feed ratio.

### 3.3. Gel retardation assays

Gel retardation assays were performed to investigate the ability of the PEI shell of PEC micelles to complex DNA via the change of EtBr fluorescence strength. When the amount of DNA was fixed at 1  $\mu$ g per unit of polyplex, the EtBr fluorescence of the pCMV-Luc band was gradually quenched as PEC micelle content increased. The weight ratios of PEC micelles to DNA at which PEC micelles can completely retard DNA are shown in Table 3. It was found that the weight ratio of PEC micelles to DNA ranged from 0.5 to 1.0 with the increase in MW of the PCL block. However, after compensating for the difference in MW of various PECs, the obtained N/P ratio of the varying PECs were all around 2.0, suggesting that the PCL block would not influence the DNA condensation of PEI. Partial DOX-loaded polymers were also examined in this study. The EtBr fluorescence disappeared at N/P ratios of 2.1, and 2.4 for DOX-PEC18 micelles and DOX-PEC55 micelles (drug/PEC ratio 1:1), respectively, which was a little higher than for PEC micelles without drug.

### 3.4. Size and zeta potential determination

As discussed above, PEC-based self-assemblies would form in an aqueous solution once the solution concentration exceeds its CMC. The sizes and zeta potentials of PEC micelles and PEC micelle/DNA complexes at various N/P ratios are listed in Table 4. The mean size of PEC18, PEC40 and PEC55 micelles were 280, 470 and 560 nm, respectively. The particle size increased with increasing MW of the hydrophobic segments in PEC, which is consistent with the previous report [28]. The particle size of DNA/PEC micelle complexes increased with N/P ratio in the range of 3 to 30 N/P ratio. All micelles presented net positive charge and the

charge increased with the increase of N/P ratio, indicating that excessive positively charged PEI covered the complex particle surface. Table 5 summarizes the particle sizes of DNA complexed with drug-loaded PEC micelles. It was observed that the micelle size increased as drug content increased for all micelles, but drug-loaded PEC40 and PEC55 micelles were smaller than the corresponding blank micelles (PEC40 micelles: 470 nm; PEC55 micelles: 560 nm) while PEC18 particles containing DOX at 1:1 drug/polymer ratio were bigger than corresponding blank micelles (PEC18 micelles: 280 nm). Drug encapsulation was supposed to exert two contrary effects on particle size. One effect is the drug may improve the compact arrangement among chains through hydrophobic interactions. The other effect is the enlargement of core bulk due to the drug content. It should be noted that the particle size change for drug-loaded PEC micelle/DNA complexes was similar to that of DNA-complexed PEC micelles without drug. Thus drug loading did not seem to hamper the capability of PEI segments in micelles to complex with DNA, which was in accordance with the gel retardant examination.

### 3.5. Cytotoxicity assay

The MTT assay was performed to evaluate the toxicity of blank micelles and drug-loaded polymeric micelles, and to investigate whether DNA influenced the cytotoxicity of polyplexes. The cytotoxicity is generally incubation time-dependent for most samples [29]. Considering the consistency of the incubation time used in gene transfection tests, the incubation time was fixed at 4 hr for this study. Compared with PEI 25K, all PEC micelles exhibited less cytotoxicity, which was in accordance with the previous study [30]. Moreover, the cytotoxicity of PEC micelles was related to their composition (Fig. 4). When 50 % cells were viable, the concentration of PEC18 micelles was about 100 $\mu$ g/mL while those of PEC40 and PEC55 micelles increased to 250 $\mu$ g/mL and 390 $\mu$ g/mL, respectively, indicating cytotoxicity decreased as increasing hydrophobic segment length for PECs. On the other side, DNA complexation seems to alleviate the cytotoxicity. For example, PEC18 polyplex at N/P ratio of 10 maintained about 100 % cell viability until the PEC18 concentration reached 62.5 $\mu$ g/mL (Fig. 5). The cytotoxicity of cationic polymers is thought to be a result of membrane damaging effects [31]. Though the micellar polyplexes were smaller than blank micelles without DNA especially for PEC40 and PEC55 (Table 4), the surface charge played a quite dominant role to influence the cytotoxicity of micellar polyplexes rather than their size. The reduction in surface charge caused by DNA complexation might weaken the electrostatic interactions between complexes and negatively charged cell surfaces, which is necessary for non-specific uptake of polyplexes [32]. Another reason was pointed out by Kim et al. [33]. The cytotoxicity associated with PEI-mediated cell transfection includes an immediate toxicity causing morphological destruction and a delayed toxicity. When PEI was complexed with DNA, the complexes showed minimal immediate toxicity. Only after PEI separates from DNA in cells can free PEI interact with cellular components and inhibit normal physical process. Thus, cell toxicity was delayed by DNA complexing.

Fig. 6 shows the influence of drug loading on cell cytotoxicity. As a control group, the live cells retained above 70% up to 20 $\mu$ g/mL free DOX. Loading DOX into the polymeric micelles rendered cytotoxicity more serious. When drug/polymer feed ratio reached 1/1, both drug-loaded PEC18 and PEC55 micelles maintained very high cell viability within the whole range of test doses. Partial explanation involves the considerable cytotoxicity caused by the polymers. For example, the drug loading content for PEC18 1/1, PEC18 1/2 and PEC18 1/4 was 23.2, 5.2 and 1.4 %, respectively. When the system contained 20 $\mu$ g/mL DOX, the corresponding polymer content was 66, 366 and 1419  $\mu$ g/mL, whose cytotoxicity should not be ignored. The restrained drug release by polymeric micelles was probably the other reason. Drug release from these systems was examined in pH5.0~7.4 PBS at 37 $^{\circ}$ C. It was found that only 16.5% DOX released from PEC55 micelles at drug/polymer feed ratios of 1/1 within 4 hr. And PEC18 systems released about 30% DOX into the outside media. In fact this delay of drug release may

be beneficial to accompanied gene transfection in this study, otherwise cells will die quickly and lose their physical function to make use of therapeutic genes.

Upon DNA complexing with DOX-loaded PEC18 and PEC55 micelles, the cell viability was enhanced significantly, which was similar to the results illustrated in Fig. 5. PEC55 complexes kept cells viable almost around 100% in all tested cases in Fig. 7(b) while the drug content and N/P ratio employed influenced the cytotoxicity of PEC18 complexes to some extent as shown in Fig. 7(a). Herein, particle size as well as surface charge should be taken into account to explain these changes upon DNA complexation.

### 3.6. Transfection efficiency

Transfection experiments were performed on HepG2 hepatocytes using PEI 25K as a control. As shown in Fig. 8(a), there is the maximum transfection efficiency vs. N/P ratio of PEC micelle/DNA complex in each plot, which was similar to the reported observation [34]. In addition, PEC18 complexes showed obviously lower transfection than PEC40 and PEC55 complexes at lower N/P ratios. The particle size and zeta potential may play a crucial role in transfection. High zeta potential of particles facilitates non-specific attachment to cells via electrostatic interactions, then induces subsequent cellular uptake. As for particle size, it seems there is an optimal value as some references reported. The particle size is smaller at low N/P ratios compared to higher N/P ratios, resulting in easy entry by endocytosis. On the other hand, the loose structure of larger particles at higher N/P ratios is beneficial to polyplex sedimentation on the cell surface and disassembly inside cells. Accordingly, the gene transfection efficiency of PEC40 and PEC55 complexes reached the highest value at N/P ratio of 6, while PEC18 curve displayed a peak at N/P ratio of 20. When cytotoxicity is taken into account, at higher N/P ratios, the increased polymer cytotoxicity hindered cell growth, and luciferase measurement tests confirmed that total protein quantity was reduced. This would cause the decrease in gene transfection efficiency as N/P ratio increased. In order to compare with the control, the original results were also expressed as the relative transfection efficiency where a value of 1 indicates equivalent transfection efficiency to PEI 25K under the same experimental conditions, shown in Fig. 8(b). Based on the combination of the above factors, the relative transfection efficiency of PEC40 and PEC55 complexes at N/P ratio of 6 achieved almost 3 times higher magnitude than that of PEI 25K.

With the goal to construct a micelle system bearing DNA and anticancer agents together, the transfection efficiency of drug-loaded polyplexes was investigated under different drug loading conditions. As seen in Fig. 9, drug content, N/P ratio and polymer type did affect gene transfection. Differences in transfection efficiency of three PEC complexes are especially pronounced in drug content. Generally high drug content (1/1) in the micelles resulted in the somewhat decrease in gene transfection. When compared to PEI 25K, however, the DOX-loaded polyplex micelles still can reach equivalent luciferase levels, even exceeding PEI 25K values up to one hundred times greater. The lowest relative gene transfection efficiency was close to 1 for PEC18 1/1 complexes, while the highest one enhanced about three orders of magnitude for PEC40 1/4 and PEC55 1/2 complexes. This result confirmed the previous assumption that drug encapsulation in the core of polymeric micelles would not hamper gene condensation and transfection. Moreover, it seems that endocytosis of the vector and gene transfection were implemented quickly before DOX exerted endocellular function.

## 4. Conclusions

A series of polycaprolactone-grafted polyethylenimine were synthesized and investigated for DOX encapsulation and gene delivery in the form of polyplex micelles. The molecular weight of PCL segments in graft polymers, drug content and N/P ratio in the system were three crucial factors that influenced the size, surface charge and inside compactness of polyplex particles,



which in turn caused differences in cytotoxicity and gene transfection of various samples. More importantly, it was indicated that drug loading didn't interfere in DNA condensation. In addition, high gene transfection efficiency of Luciferase was achieved under the given condition in HepG2 cells. Therefore, this group of cationic graft polymers may be useful to conquer MDR problem using the concept of synergistic effects of drug and gene therapy.

## Acknowledgments

This work is partially supported by NIH CA101850.

## References

1. Twaites BR, de las Heras Alarcon C, Cunliffe D, Lavigne M, Pennadam S, Smith JR, Gorecki DC, Alexander C. Thermo and pH responsive polymers as gene delivery vectors: effect of polymer architecture on DNA complexation in vitro. *J Control Rel* 2004;97:551–66.
2. Sethuraman VA, Na K, Bae YH. pH-Responsive sulfonamide/PEI system for tumor specific gene delivery: an in vitro study. *Biomacromol* 2006;7:64–70.
3. Bennis S, Chapey, Robert J, Couvreur P. Enhanced cytotoxicity of doxorubicin encapsulated in polyisohexylcyanoacrylate nanospheres against multidrug-resistant tumour cells in culture. *European J Cancer* 1994;30(1):89–93. [PubMed: 8142172]
4. Cuvier C, Roblot-Treupel L, Millot JM, Lizard G, Chevillard S, Manfait M, Couvreur P, Poupon MF. Doxorubicin-loaded nanospheres bypass tumor cell multidrug resistance. *Biochem Pharmacology* 1992;44(3):509–517.
5. Barraud L, Merle P, Soma E, Lefrancois L, Guerret S, Chevallier M, Dubernet C, Couvreur P, Trépoil C, Vitvitski L. Increase of doxorubicin sensitivity by doxorubicin-loading in nanoparticles for hepatocellular carcinoma cells in vitro and in vivo. *J Hepatology* 2005;42:736–743.
6. Vauthier C, Dubernet C, Chauvierre C, Brigger I, Couvreur P. Drug delivery to resistant tumors: the potential of poly(alkyl cyanoacrylate) nanoparticles. *J Contr Release* 2003;93:151–160.
7. Kabanov AV, Batrakova EV, Alakhov VY. Pluronic block copolymers as novel polymer therapeutics for drug and gene delivery. *J Contr Release* 2002;82:189–212.
8. Kabanov AV, Batrakova EV, Alakhov VY. An essential relationship between ATP depletion and chemosensitizing activity of Pluronic block copolymers. *J Contr Release* 2003;91:75–83.
9. Kabanov AV, Batrakova EV, Alakhov VY. Pluronic block copolymers for overcoming drug resistance in cancer. *Adv Drug Deliv Rev* 2002;54:759–779. [PubMed: 12204601]
10. Mamot C, Drummond DC, Hong K, Kirpotin DB, Park JW. Liposome-based approaches to overcome anticancer drug resistance. *Drug Resistance Updates* 2003;6(5):271–279. [PubMed: 14643297]
11. Kobayashi T, Ishida T, Okada Y, Ise S, Harashima H, Kiwada H. Effect of transferrin receptor-targeted liposomal doxorubicin in P-glycoprotein-mediated drug resistant tumor cells. *Inter J Pharm* 2007;329:94–102.
12. Kobayashi H, Takemura Y, Wang FS, Oka T, Ohnuma T. Retrovirus-mediated transfer of anti-MDR1 hammerhead ribozymes into multidrug-resistant human leukemia cells: screening for effective target sites. *Int J Cancer* 1999;81:944–50. [PubMed: 10362143]
13. Gao ZQ, Gao ZP, Fields JZ, Boman BM. Tumor-specific expression of anti-mdr1 ribozyme selectively restores chemosensitivity in multidrug-resistant colon-adenocarcinoma cells. *Int J Cancer* 1999;82:346–52. [PubMed: 10399951]
14. Sampath J, Sun D, Kidd VJ, Grenet J, Gandhi A, Shapiro LH, Wang QJ, Zambetti GP, Schuetz JD. Mutant p53 cooperates with ETS and selectively up-regulates human MDR1 not MRP1. *J Biol Chem* 2001;276:39359–67. [PubMed: 11483599]
15. Zhan MC, Yu DH, Lang AQ, Li L, Pollock RE. Wild type p53 sensitizes soft tissue sarcoma cells to doxorubicin by down-regulating multidrug resistance-1 expression. *Cancer* 2001;92:1556–66. [PubMed: 11745235]
16. Stein U, Walther W, Shoemaker RH. Reversal of multidrug resistance by transduction of cytokine gene into human colon carcinoma cells. *J Natl Cancer Inst* 1996;88:1383–92. [PubMed: 8827016]

17. Wang Y, Gao S, Ye WH, Yoon HS, Yang YY. Co-delivery of drugs and DNA from cationic core-shell nanoparticles self assembled from a biodegradable copolymer. *Nature Materials*. Published online 24 Sept. 2006
18. Wightman L, Kircheis R, Rossler V, Carotta S, Ruzicka R, Kurska M, Wagner E. Different behavior of branched and linear polyethylenimine for gene delivery in vitro and in vivo. *J Gene Med* 2001;3:362–372. [PubMed: 11529666]
19. Yang C, Li HZ, Goh SH, Li J. Cationic star polymers consisting of  $\alpha$ -cyclodextrin core and oligoethylenimine arms as nonviral gene delivery vectors. *Biomaterials* 2007;28:3245–3254. [PubMed: 17466370]
20. Meran T, Kopeček J, Kissel T. Prospects for cationic polymers in gene and oligonucleotide therapy against cancer. *Adv Drug Deliv Rev* 2002;54:715–758. [PubMed: 12204600]
21. Wang CH, Hsiue GH. Polymer-DNA hybrid nanoparticles based on folate-polyethylenimine-block-poly(L-lactide). *Bioconj Chem* 2005;16:391–6.
22. Shuai XT, Merdan T, Unger F, Wittmar M, Kissel T. Novel biodegradable ternary copolymers hy-PEI-g-PCL-b-PEG: synthesis, characterization, and potential as efficient nonviral gene delivery vectors. *Macromol* 2003;36:5751–9.
23. Zhang JX, Qiu LY, Zhu KJ, Jin Y. Thermally responsive polymeric micelles self-assembled by poly (N-isopropylacrylamide) grafted polyphosphazene: synthesis, characterization and in vitro drug release study. *J Biomed Mater Res A* 2006;76:773–80. [PubMed: 16345095]
24. Kataoka K, Matsumoto T, Yokoyama M, Okano T, Sakurai Y, Fukushima S, Okamoto K, Kwon GS. Doxorubicin-loaded poly(ethylene glycol)-poly(b-benzyl-L-aspartate) copolymer micelles: their pharmaceutical characteristics and biological significance. *J Control Rel* 2000;64:143–53.
25. Wilhelm M, Zhao CL, Wang Y, Xu R, Winnik MA. Poly (styrene-ethylene oxide) block copolymer micelle formation in water: a fluorescence probe study. *Macromol* 1991;24:1033–40.
26. Domeselaar GHV, Kwon GS, Andrew LC, Wishart DS. Application of solid phase peptide synthesis to engineering PEO-peptide block copolymers for drug delivery. *Colloids and Surf B: Biointerfaces* 2003;30:323–34.
27. Kohori F, Yokoyama M, Sakai K, Okano T. Process design for efficient and controlled drug incorporation into polymeric micelle carrier systems. *J Control Rel* 2002;78:155–63.
28. Allen C, Maysinger D, Eisenberg A. Nano-engineering block copolymer aggregates for drug delivery. *Colloids Surf B: Biointerfaces* 1999;16:3–27.
29. Kang HC, Kim SW, Lee MY, Bae YH. Polymeric gene carrier for insulin secreting cells: Poly(L-lysine)-g-sulfonyleurea for receptor mediated transfection. *J Control Rel* 2005;105:164–76.
30. Kunath K, Harpe AV, Fischer D, Kissel T. Galactose-PEI-DNA complexes for targeted gene delivery: Degree of substitution affects complex size and transfection efficiency. *J Control Rel* 2003;88:159–72.
31. Kunath K, Harpe AV, Fischer D, Petersen H, Bickel U, Voigt K, Kissel T. Low-molecular-weight polyethylenimine as a non-viral vector for DNA delivery: comparison of physicochemical properties, transfection efficiency and in vivo distribution with high-molecular-weight polyethylenimine. *J Control Rel* 2003;89:113–25.
32. Mislick KA, Baldeschwieler JD. Evidence for the role of proteoglycans in cation-mediated gene transfer. *Proc Natl Acad Sci USA* 1996;93:12349–54. [PubMed: 8901584]
33. Kim YH, Park JH, Lee MH, Kim YH, Park TG, Kim SW. Polyethylenimine with acid-labile linkages as a biodegradable gene carrier. *J Control Rel* 2005;103:209–19.
34. Chiu SJ, Ueno NT, Lee RJ. Tumor-targeted gene delivery via anti-HER2 antibody (trastuzumab, Herceptin<sup>®</sup>) conjugated polyethylenimine. *J Control Rel* 2004;97:357–69.

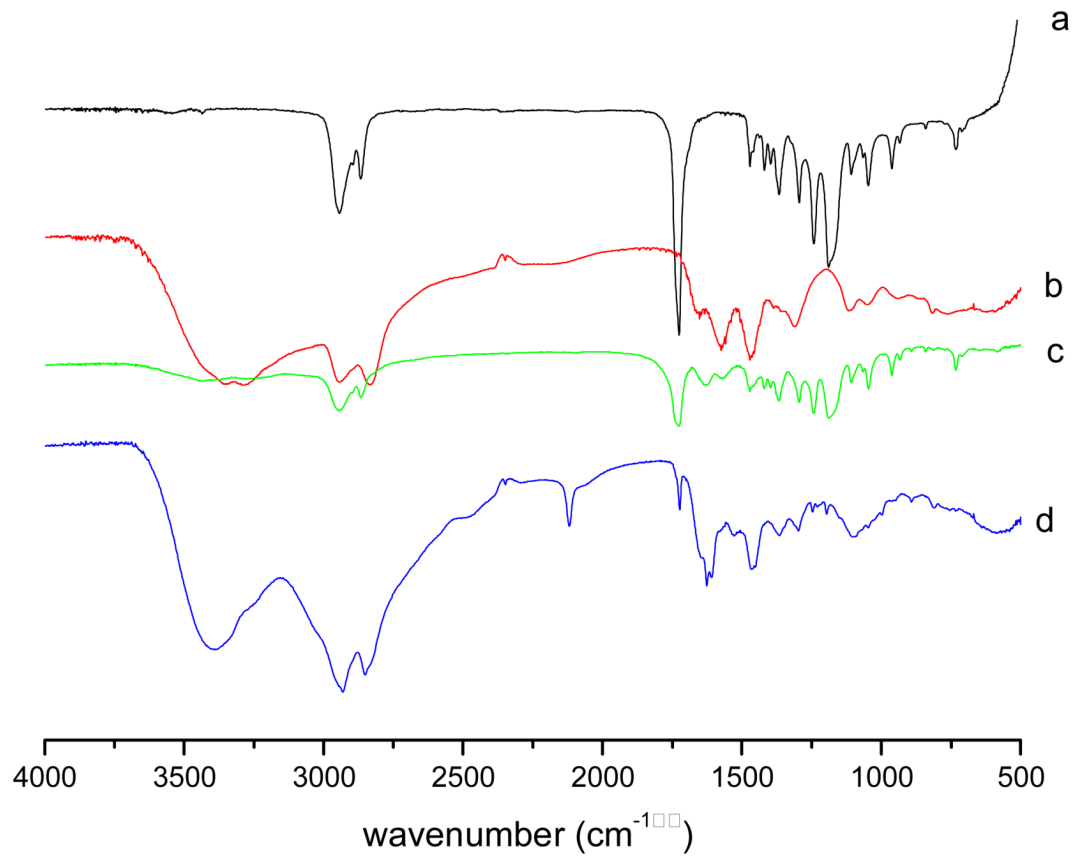


**Fig. 1.** FTIR spectra of (a) PCL-OH; (b) PEI 1800; (c) PEC which did not dissolve in methanol and (d) PEC which can dissolve in methanol.

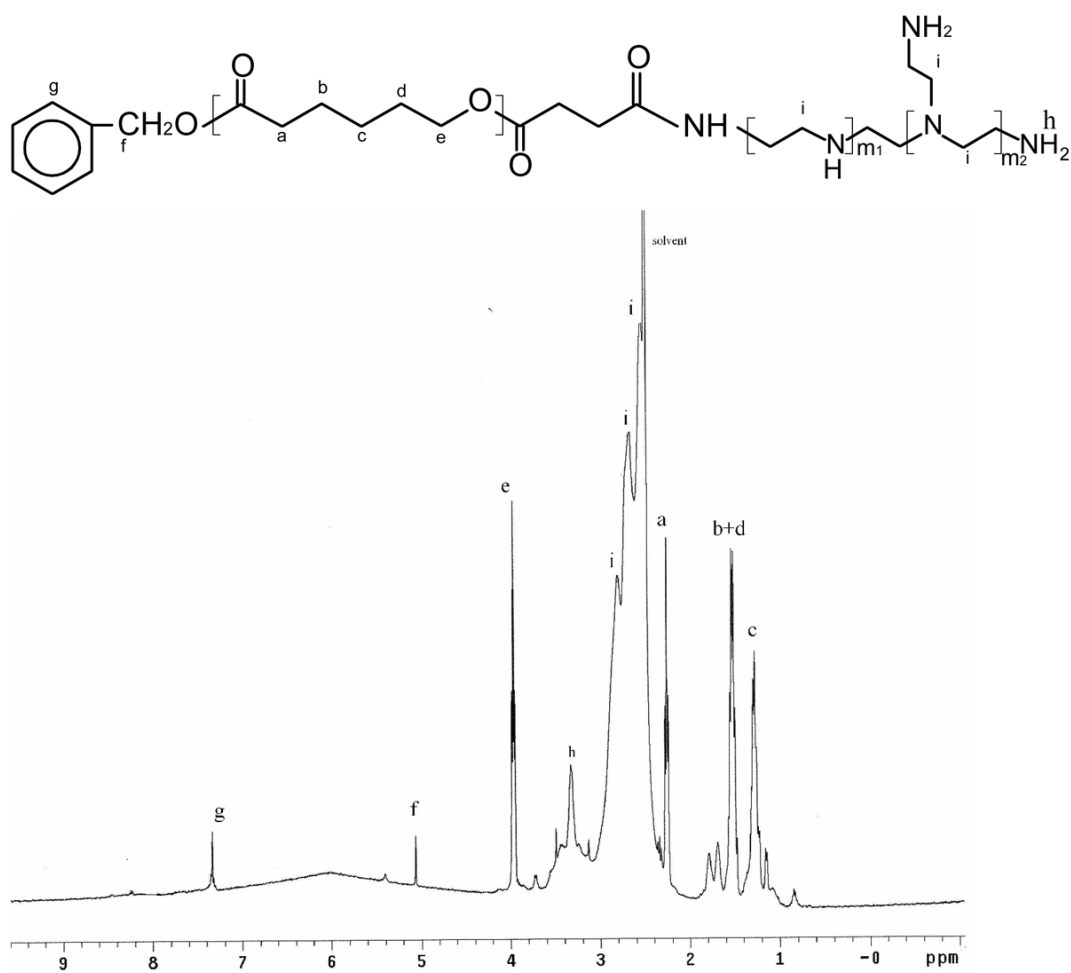


**Fig. 2.**  
<sup>1</sup>H NMR spectrum of PEC18 in d<sub>6</sub>-DMSO.

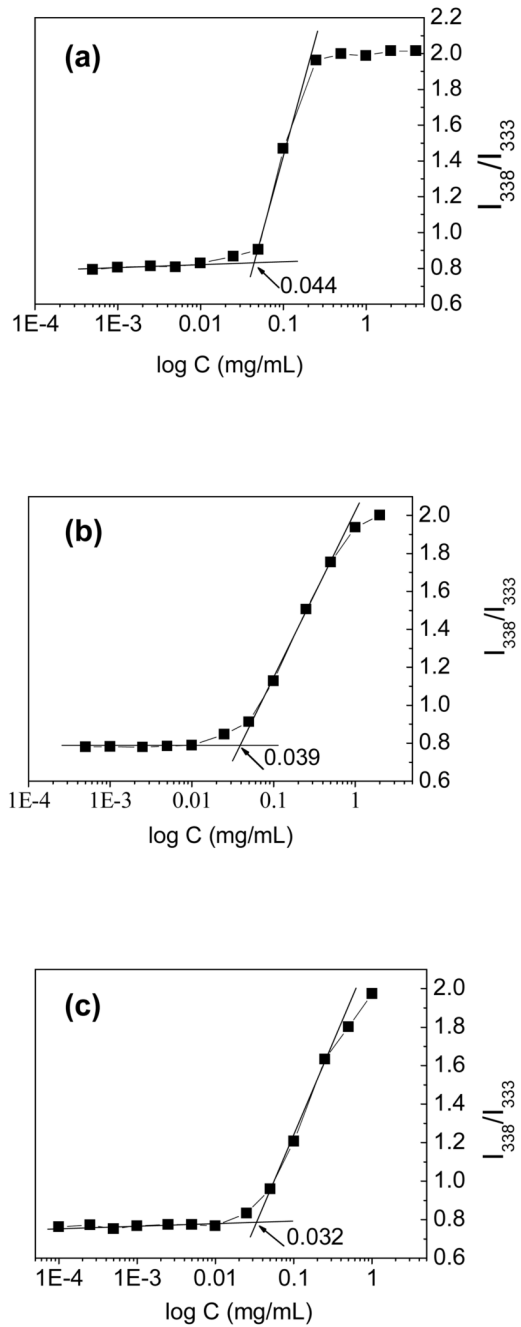


**Fig. 3.** Plots of the intensity ratio  $I_{338}/I_{333}$  (from pyrene excitation spectra at  $\lambda_{em}=390$  nm) vs.  $\log C$  for (a)PEC18, (b)PEC40 and (c)PEC55 with various compositions.



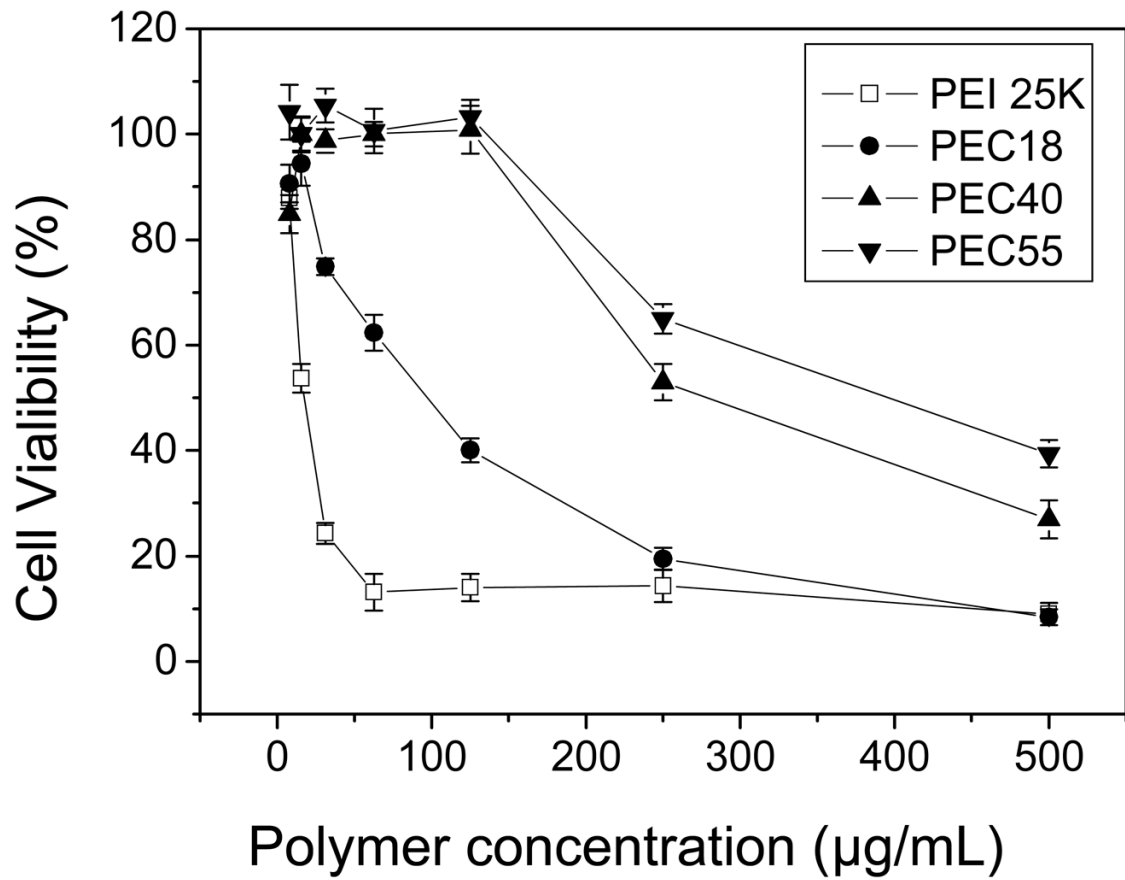


**Fig. 4.** Cell viability upon addition of increasing concentration of PEI 25K and PEC to HepG2 cells after 4 hr incubation (n=6).

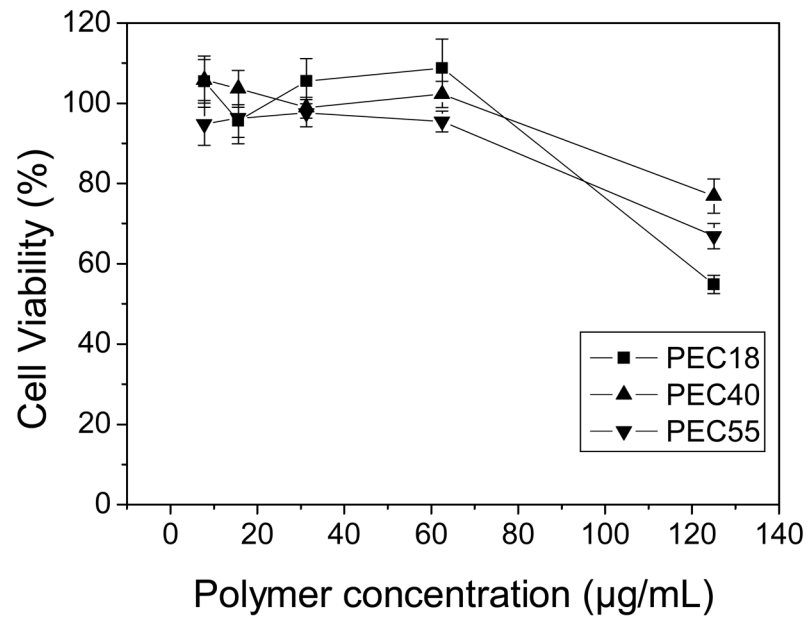


**Fig. 5.** Cell viability upon addition of increasing concentration of DNA complexed PEC to HepG2 cells after 4 hr incubation at N/P ratio of 10 (n=6).

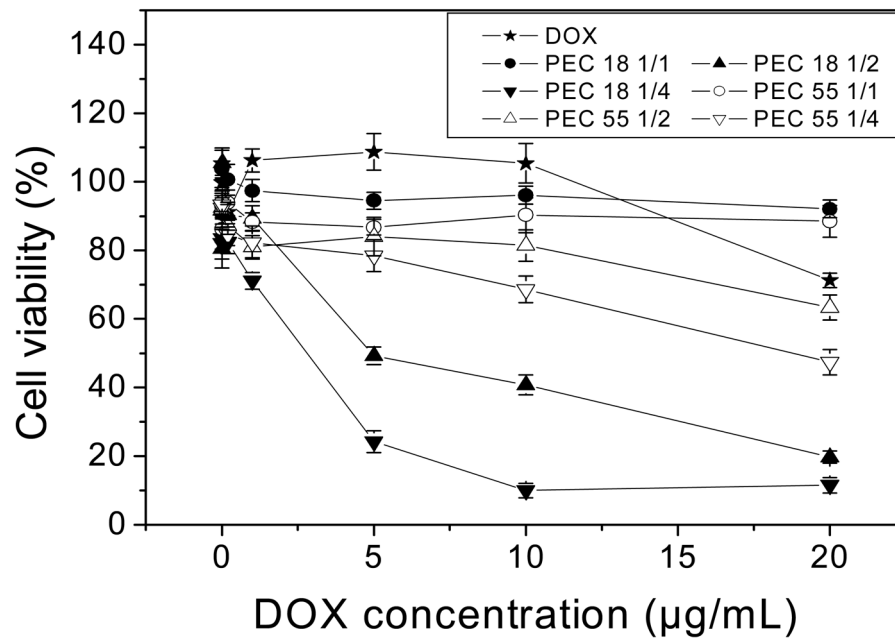


**Fig. 6.** Cell viability of DOX, DOX-loaded PEC18 and DOX-loaded PEC55 at various feed ratio of drug to polymer (n=6).

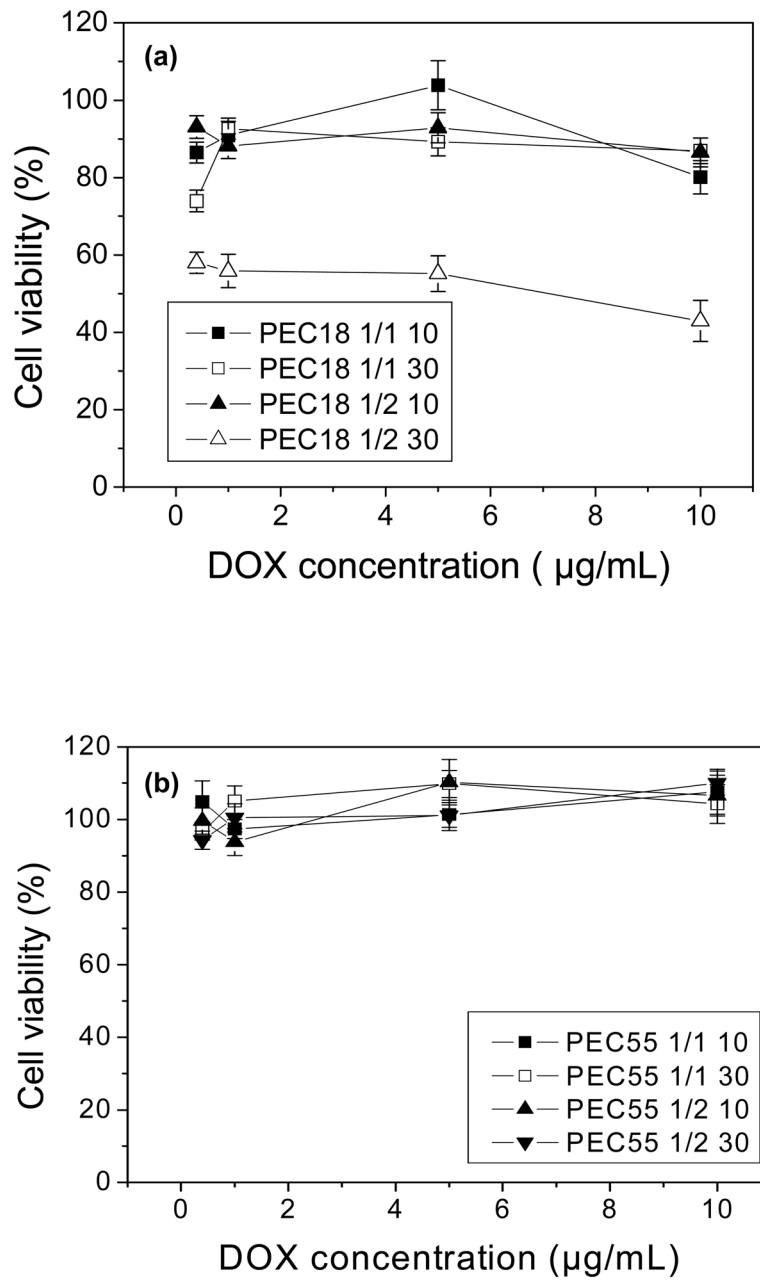


**Fig. 7.** Cell viability of DOX-loaded PEC18 and PEC55 at N/P ratio of 10 and 30 (n=6).

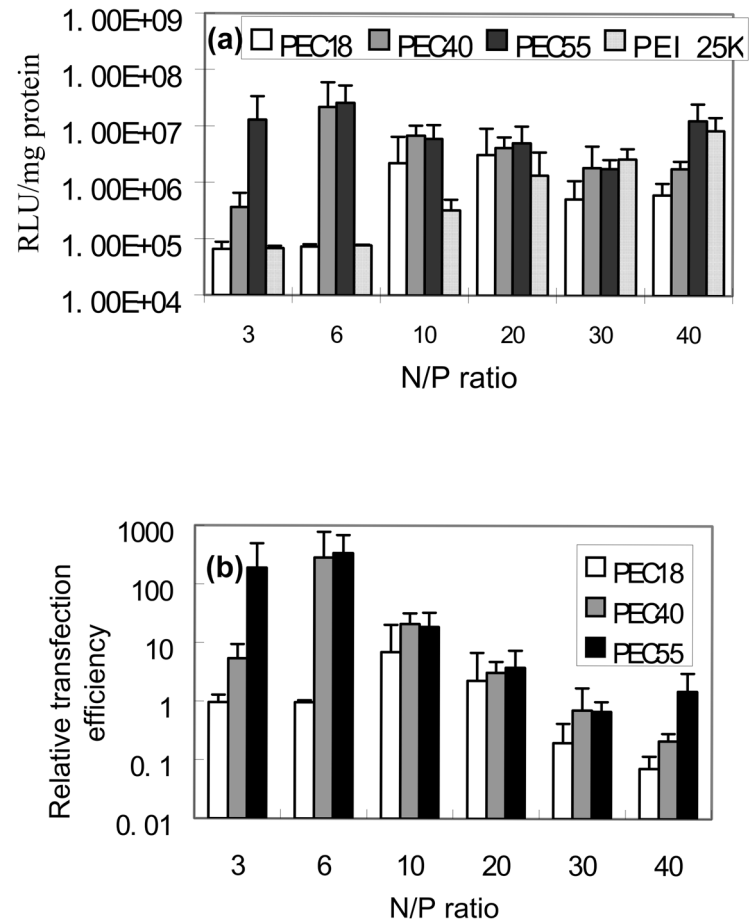


**Fig. 8.** (a) Gene transfection of PEI 25K and PEC/DNA complexes with HepG2 cells and (b) Relative gene transfection efficiency of complexes (n=4).



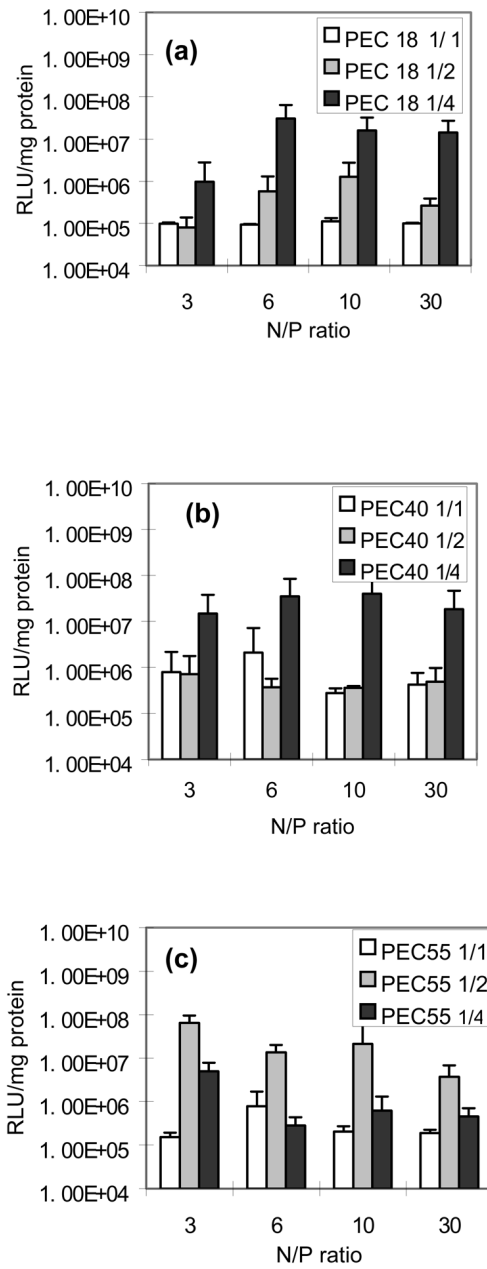
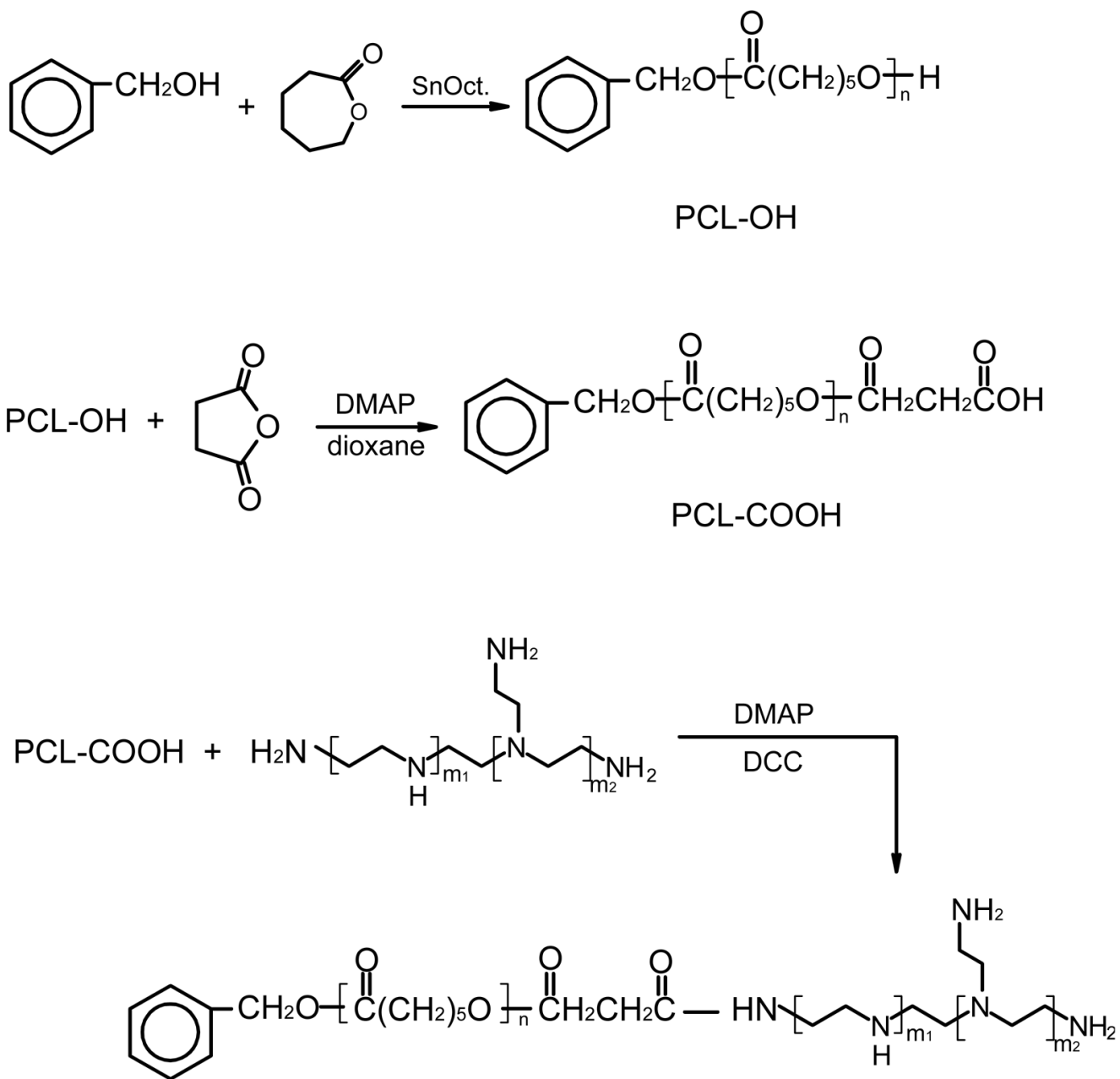


**Fig. 9.** Gene transfection efficiencies of DOX-loaded PEC/DNA complexes with HepG2 cells using PEI 25K as control: (a)PEC18, (b)PEC40 and (c)PEC55 (n=4).



**Scheme 1.**  
Synthesis route of branched PEI-graft-PCL (PEC)

Table 1

Characteristics of PEI-*graft*-PCL (PEC) copolymers.

Polymer	Feed molar ratio of CL to BA	MW of PCL-OH <sup>a</sup>	Graft ratio <sup>b</sup>	MW	
				Theo. Value <sup>c</sup>	Exp. Value <sup>d</sup>
PEC18	5	1800	0.85	3330	3990
PEC40	10	4000	0.84	5160	5220
PEC55	15	5500	0.75	5930	6440

<sup>a</sup>The molecular weight of PCL-OH was calculated from <sup>1</sup>H NMR spectra;

<sup>b</sup>The graft ratio of PEC was calculated from <sup>1</sup>H NMR spectra;

<sup>c</sup>Theory value of MW was calculated from graft ratio of PEC;

<sup>d</sup>Experimental value was obtained from GPC analysis.

**Table 2**

The drug loading content DOX-encapsulated PEC micelle at various drug/polymer feed ratios.

PEC micelle	Drug/polymer feed ratio (w/w)	Drug loading content (%)
PEC18 micelle	1/4	1.4
	1/2	5.2
	1/1	23.2
PEC40 micelle	1/4	0.7
	1/2	2.2
	1/1	20.4
PEC55 micelle	1/4	3.4
	1/2	5.7
	1/1	20.2

**Table 3**

Weight ratio of PEC micelle to DNA and N/P ratio when PEC micelles (with or without drug) complex with DNA completely.

Micelle	Weight ratio of PEC micelle to DNA	N/P ratio
PEC18 micelle	0.5	2.0
PEC40 micelle	0.8	2.0
PEC55 micelle	1.0	2.2
DOX-PEC18 (1/1) <sup>a</sup> micelle	0.5	2.1
DOX-PEC55 (1/1) micelle	1.1	2.4

<sup>a</sup>The number in the bracket presents the feed ratio of drug to polymer (w/w).



**Table 4**

The effect of N/P ratio on particle size and zeta potential DNA/PEC complexes.

PEC micelle	N/P ratio	Particle size (nm)	Zeta potential (mV)
PEC18 micelle	none <sup>a</sup>	280	29
	3	200	16
	6	250	18
	10	260	18
	30	330	20
	PEC40 micelle	none <sup>a</sup>	470
PEC40 micelle	3	210	13
	6	230	19
	10	280	18
	30	310	22
	PEC55 micelle	none <sup>a</sup>	560
PEC55 micelle	3	180	12
	6	240	20
	10	260	19
	30	320	23

<sup>a</sup> without DNA

**Table 5**  
The effect of drug loading and N/P ratio on the size of DNA/PEC micelle complex particle.

PEC micelle	N/P ratio			
	none <sup>a</sup>	3	10	30
DOX-PEC18 1/4 micelle	230	170	220	280
DOX-PEC18 1/2 micelle	260	200	240	280
DOX-PEC18 1/1 micelle	320	270	310	390
DOX-PEC40 1/4 micelle	270	150	200	230
DOX-PEC40 1/2 micelle	300	170	250	290
DOX-PEC40 1/1 micelle	380	200	300	320
DOX-PEC55 1/4 micelle	250	220	260	240
DOX-PEC55 1/2 micelle	260	220	220	310
DOX-PEC55 1/1 micelle	330	180	280	310

<sup>a</sup> without DNA